

# Activity estimation in radioimmunotherapy using magnetic nanoparticles

Samira Rasaneh<sup>1</sup>, Hossein Rajabi<sup>2</sup>, Fariba Johari Daha<sup>1</sup>

<sup>1</sup>Department of Radioisotope, Nuclear science and Technology Research Institute, Tehran 14115-331, Iran; <sup>2</sup>Department of Medical Physics, School of Medical Sciences, Tarbiat Modares University, Tehran 14115-331, Iran

Correspondence to: Samira Rasaneh. Department of Radioisotope, Nuclear science and Technology Research Institute, Tehran 14115-331, Iran. Email: srasaneh@aeoi.org.ir.

**Objective:** Estimation of activity accumulated in tumor and organs is very important in predicting the response of radiopharmaceuticals treatment. In this study, we synthesized <sup>177</sup>Lutetium (<sup>177</sup>Lu)-trastuzumab-iron oxide nanoparticles as a double radiopharmaceutical agent for treatment and better estimation of organ activity in a new way by magnetic resonance imaging (MRI).

**Methods:** <sup>177</sup>Lu-trastuzumab-iron oxide nanoparticles were synthesized and all the quality control tests such as labeling yield, nanoparticle size determination, stability in buffer and blood serum up to 4 d, immunoreactivity and biodistribution in normal mice were determined. In mice bearing breast tumor, liver and tumor activities were calculated with three methods: single photon emission computed tomography (SPECT), MRI and organ extraction, which were compared with each other.

**Results:** The good results of quality control tests (labeling yield: 61%±2%, mean nanoparticle hydrodynamic size: 41±15 nm, stability in buffer: 86%±5%, stability in blood serum: 80%±3%, immunoreactivity: 80%±2%) indicated that <sup>177</sup>Lu-trastuzumab-iron oxide nanoparticles could be used as a double radiopharmaceutical agent in mice bearing tumor. Results showed that <sup>177</sup>Lu-trastuzumab-iron oxide nanoparticles with MRI had the ability to measure organ activities more accurate than SPECT.

**Conclusions:** Co-conjugating radiopharmaceutical to MRI contrast agents such as iron oxide nanoparticles may be a good way for better dosimetry in nuclear medicine treatment.

**Keywords:** Radioimmunotherapy (RIT); activity estimation; lutetium-177; herceptin; magnetic nanoparticles; magnetic resonance imaging (MRI)

Submitted Jul 08, 2014. Accepted for publication Dec 11, 2014.

doi: 10.3978/j.issn.1000-9604.2015.03.06

View this article at: <http://dx.doi.org/10.3978/j.issn.1000-9604.2015.03.06>

## Introduction

In recent years, targeted radioimmunotherapy (RIT) using monoclonal antibodies directed to cancer cell surface antigens has been clinically validated (1-4). In RIT, antibodies are labeled with radioisotopes and used for localization and therapy of cancer (5). There is now a preponderance of evidence to suggest that RIT will be most successful in the treatment of micrometastatic disease (6).

Calculation of the energy delivered to critical organs and tumors is essential to predict both organ toxicity and tumor response. The current practice (7) to perform dosimetry is combination planar whole-body imaging to determine

absolute activity in the organs and medical internal radiation dose (MIRD) S-factor tables derived from five anthropomorphic phantom models (8).

A limit of this approach is the inaccuracy of activity measurements obtained from planar imaging (9). Organ dosimetry requires multiple views, the often highly subjective practice of drawing of regions of interest around organs, estimates of organ volume, calculation of fractional energy deposition in organs, difficult to correct background counts, attenuation correction, and scatter correction (9,10).

Magnetic resonance imaging (MRI) and computed tomography (CT) are high-resolution modalities that

can be used to provide the anatomical information for dosimetry and treatment planning, however, their image sensitivity is lower than that of single photon emission computed tomography (SPECT) (11-13). An idea to solve the problems is to use a high-resolution modality (e.g., MRI) for direct imaging of the radiopharmaceutical agents.

We have already synthesized  $^{177}\text{Lu}$ -trastuzumab as a radiopharmaceutical agent for RIT of breast cancer and performed some preliminary studies (14,15). In the present study, we conjugated  $^{177}\text{Lu}$ -trastuzumab to iron oxide nanoparticles. This type of magnetic nanoparticles is routinely used as a negative contrast agent in MRI and can improve the sensitivity of this modality (16,17). It was investigated whether the activity distribution of  $^{177}\text{Lu}$ -trastuzumab-iron oxide nanoparticles in organs can be determined more accurately by MRI.

## Materials and methods

### Reagents and chemicals

Trastuzumab, a humanized IgG1 monoclonal antibody directed against human epidermal growth factor receptor 2 (HER2), was purchased in 150 mg vial from Genentech Inc. (South San Francisco, USA). 1,4,7,10-Tetraazacyclododecane-1,4,7,10-tetraacetic acid (DOTA) was prepared from Macroyclic Company, and other chemical agents were purchased from Sigma.

### Mice bearing breast tumor

The tumor was originally established from a spontaneous breast tumor (a murine mammary carcinoma) in an inbred female BALB/c mouse. The breast tumor model was established by subcutaneous implantation of the tumor fragments (about 1 mm<sup>3</sup>) in the right flank region of normal inbred female BALB/c mice (20-25 g, 8-10 weeks old). The biodistribution and imaging study was performed in the mice bearing breast tumors. The interaction of trastuzumab on tumor cells was assessed by immunohistochemistry (18). Animal experiments were performed in compliance with the regulation of our institution and with generally accepted guidelines governing such work.

### Conjugation of trastuzumab-DOTA to magnetic nanoparticles

Trastuzumab was conjugated to DOTA according to the Yordanov method (13). Dextran-coated iron oxide

nanoparticles were prepared using co-precipitation method that described completely before (16,17).

Sodium meta-periodate (30 mg) was added to iron oxide nanoparticles (1,400 mg) in citrate buffer (2 mL, 0.02 mol/L) and incubated for 5 h in the dark place. Trastuzumab-DOTA (200 mg) was added to the activated nanoparticle solution and incubated at 4 °C for 16 h. The mixture was deoxidized by adding sodium cyanoborohydride at 4 °C for 2 h.

### Radiolabeling of DOTA-trastuzumab-nanoparticles with $^{177}\text{Lu}$

$^{177}\text{LuCl}_3$  (5 mCi, with typical specific activity 20 Ci/mg) was added to trastuzumab-DOTA-nanoparticles (150 µg) in ammonium acetate buffer (0.25 mol/L, pH =7.0) and heated for 3 h at 37 °C. The complex was purified by gel filtration on Sephadex G-25 column. The last Fe (mg)/activity (mCi) ratio was determined (13-17).

### Quality control tests

The size distribution of the nanoparticles was analyzed using Zeta Sizer 3000HS (Malvern, UK). The core size of nanoparticles was determined by transmission electronic microscopy (TEM) (JEM 2010, JEOL, Japan). Labeling yield of the last complex ( $^{177}\text{Lu}$ -trastuzumab-nanoparticle) was analyzed by instant thin layer chromatography (ITLC) (14,15). The stability of the complex in phosphate buffer and human blood serum up to 7 d was determined (14). The immunoreactivity of the complex on SKBr3 cells was also checked based on the method described by Lindmo *et al.* (19). SKBr3 cells are hormone-independent cells originally derived from a breast adenocarcinoma expressing high levels of HER2 (20).

The biodistribution study was performed in mice bearing breast tumor at 4 and 24 h post injection [300 µCi, 100 µg (Fe)/0.1 mL] of  $^{177}\text{Lu}$ -trastuzumab-nanoparticle and  $^{177}\text{Lu}$ -trastuzumab to find the difference between their biodistributions.

### Activity determination by MRI

$^{177}\text{Lu}$ -trastuzumab-nanoparticles [300 µCi, 100 µg (Fe)/0.1 mL] were injected intravenously into 20 mice bearing breast tumors and randomly divided into four groups (n=5). At 1, 3, 5 and 7 d post injection, the animals were anesthetized (using combination of xylazine hydrochloride and ketamine hydrochloride). Imaging was performed with 1.5 Tesla MRI system (Siemens, Symphony) and a knee coil. All animals

**Table 1** The complex (Fe<sub>3</sub>O<sub>4</sub>:trastuzumab:<sup>177</sup>Lu) characteristics at pH=7

Characteristic	Value
Iron/antibody molar ratio	3.1-3.5
Nanoparticle core size (nm), $\bar{x}\pm s$	9.0±0.5
Nanoparticle hydrodynamic size (nm), $\bar{x}\pm s$	41±15
Total amount of Fe (μg):Lu (μCi)	1:3

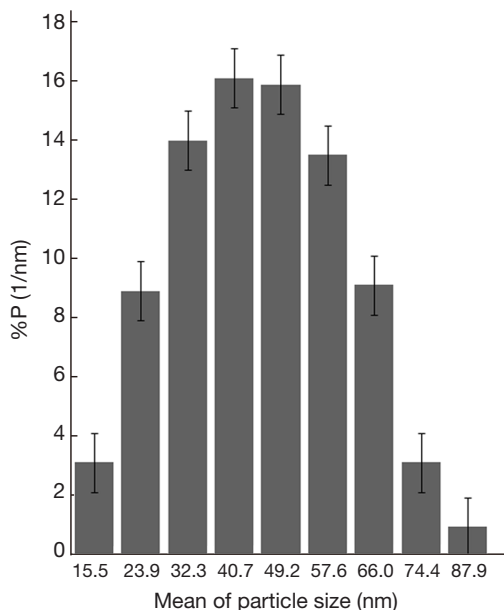


**Figure 1** Nanoparticle size distribution determined by DLS technique with the mean of 41±15 nm. DLS, dynamic light scattering.

were scanned by a fast gradient echo pulse sequence (TR =3,000, TE =90, flip angle =10°) in 288×384 matrix size. Measurements of signal intensities (liver and tumor) were performed directly on the T2 images using an operator-defined region of interest (ROI) with a constant size of pixels. The relative change in signal intensity before  $SI_{before}$  and after administration of the complex with the complex  $SI_{after}$  was calculated as follows:

$$\text{Enhancement} = 100 \times \frac{SI_{before} - SI_{after}}{SI_{before}}$$

The relation between iron content in organs and enhancement in images was obtained by imaging from a phantom with definite concentration of iron oxide nanoparticles. The mean tumor and liver volumes were determined from MRI images. After calculation of iron

content in each organ, the activity was evaluated by the complex Fe (mg)/Lu (mCi) ratio.

**Activity determination by SPECT imaging**

After MRI, each mouse was scanned using a small field-of-view SPECT (E.cam, Siemens Medical Systems) equipped with a low-energy, high-resolution collimator (LEHR). The images were recorded with 550,000 counts and in matrix size of 256×256. The energy windows were set to 113±11 keV and 208±21 keV to limit the main  $\gamma$ -photons of <sup>177</sup>Lu. After reconstruction, the computer-assisted ROI technique was applied to estimate the counts presenting in livers and tumors as described by van Reenen *et al.* (21). Considering the sensitivity of SPECT system, the mean liver and tumor activity was calculated for each mouse.

**Activity determination by tissue extraction**

When imaging was completed, the animals were killed by CO<sub>2</sub> gas and dissected. The livers and tumors were removed, weighed and counted for <sup>177</sup>Lu using a dual-channel automated gamma counter (ORTEC EG&G).

**Statistical analysis**

SPSS package (version 13.0, SPSS Inc., Chicago, IL, USA) was used for statistical analyses. For all the tests, P<0.05 was considered as statistically significant. Student’s *t*-test was used to analyze the activity estimation data point by point.

**Results**

**Quality control tests**

The complex characteristics are summarized in *Table 1*. The mean hydrodynamic size of the nanoparticles was 41±15 nm by dynamic light scattering (DLS) technique (the data are shown in *Figure 1*) and the average core size was 9.0±2.5 nm. The labeling yield and immunoreactivity were 61%±2% and 80%±2% respectively. On average, 86%±5% and 80%±3% of <sup>177</sup>Lu-trastuzumab were stable in phosphate buffer and in human blood serum up to 7 d, respectively. Nanoparticle-trastuzumab was stable in phosphate buffer up to 8 d. The size increasing was only 4% and no free trastuzumab was measurable in phosphate buffer saline (PBS) at this period.

The biodistribution study of <sup>177</sup>Lu-trastuzumab and

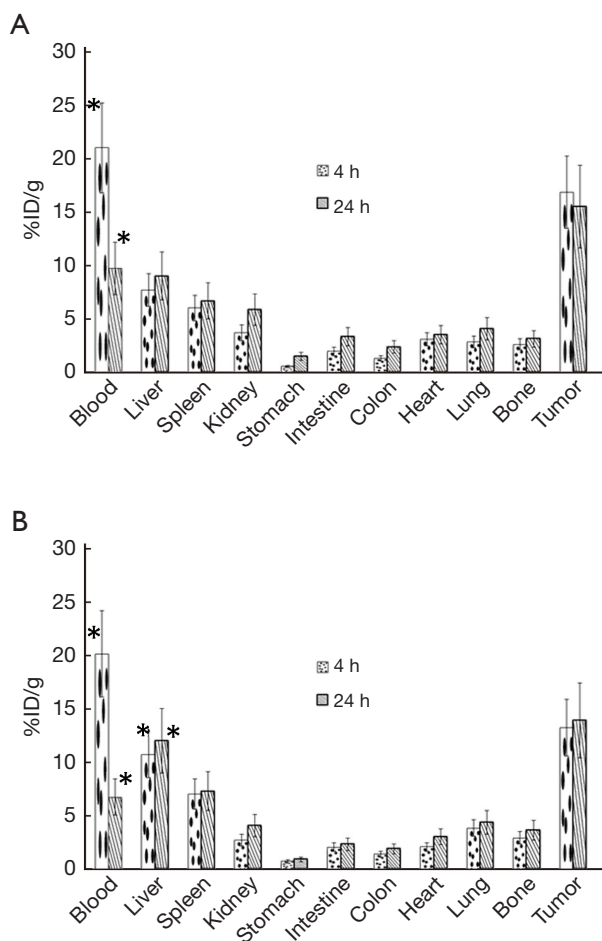


**Figure 2** The comparison biodistribution of  $^{177}\text{Lu}$ -trastuzumab (A) and  $^{177}\text{Lu}$ -trastuzumab-nanoparticles (B) in mice bearing breast tumor.

$^{177}\text{Lu}$ -trastuzumab-nanoparticles was performed in mice bearing breast tumor and the comparison results are shown in *Figure 2*. As can be seen,  $^{177}\text{Lu}$ -trastuzumab-nanoparticles aggregated in liver more (about 7%) than  $^{177}\text{Lu}$ -trastuzumab but there was no specific accumulation in other organs ( $P < 0.05$ ).

### Activity determination

The immunohistochemistry results showed the spontaneous breast tumor that we used in this study expressed medium levels of HER2. The MRI and SPECT images of a representative mouse before and after administration of the complex are presented in *Figure 3* and *Figure 4* respectively. The MRI image of phantom with definite concentration

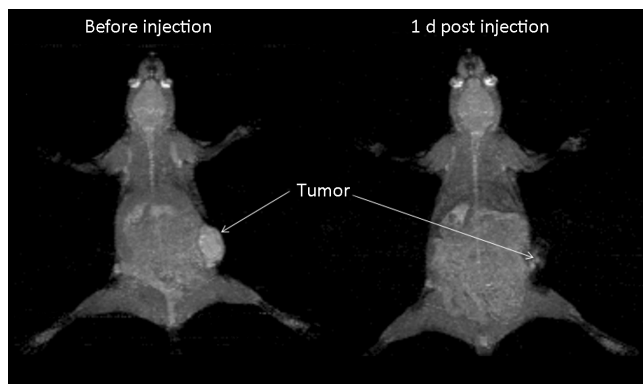


**Figure 3** The MRI images before and 1 d after injection of the complex (100  $\mu\text{g}$  Fe). MRI, magnetic resonance imaging.

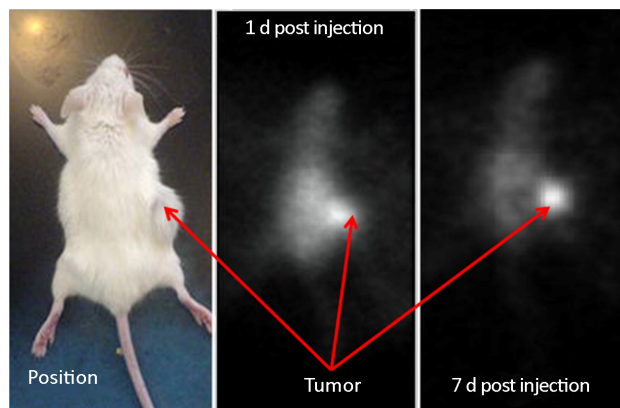


**Figure 4** The SPECT images at 1 and 7 d post injection of the complex (300  $\mu\text{Ci}$  Lu). The arrows show the tumors. SPECT, single photon emission computed tomography.

of iron oxide nanoparticles and its calibration curve are shown in *Figure 5*. The mean activity in tumor and liver determined by three methods are presented in *Table 2*. As can be seen, the activity calculation using MRI images was nearer to real amounts than that using SPECT images. The standard deviation amounts in activity estimation by MRI was statistically lower than that by SPECT ( $P < 0.05$ ).

### Discussion

In RIT, accurate estimation of the dose delivered to metastatic tumors and critical organs is essential for treatment planning and predicting RIT response (5,22). Accurate dose estimation requires exact measurements of organ volume and radiopharmaceutical content (8,22).

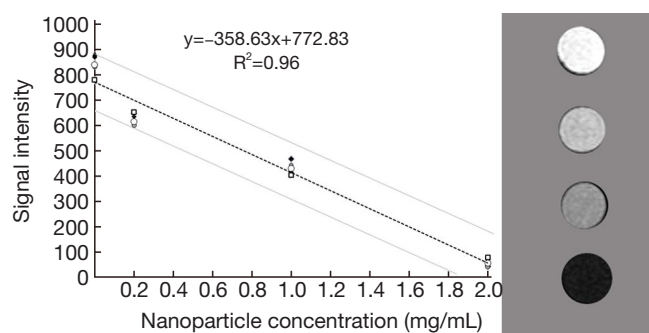


**Figure 5** The MRI image of phantom with definite concentration of iron oxide nanoparticles and its calibration curve. MRI, magnetic resonance imaging.

**Table 2** The activity ( $\bar{x} \pm s$ ) in tumor and liver determined by three different methods at 1, 3, 5 and 7 d post injection of the complex

Organ	Tissue extraction ( $\mu\text{Ci}$ )	SPECT ( $\mu\text{Ci}$ )	MRI ( $\mu\text{Ci}$ )*
Liver (1 d)	51 $\pm$ 10	68 $\pm$ 27	45 $\pm$ 13
Tumor (1 d)	61 $\pm$ 11	81 $\pm$ 30	50 $\pm$ 19
Liver (3 d)	48 $\pm$ 9	64 $\pm$ 24	41 $\pm$ 17
Tumor (3 d)	84 $\pm$ 15	96 $\pm$ 37	74 $\pm$ 23
Liver (5 d)	37 $\pm$ 10	47 $\pm$ 21	31 $\pm$ 12
Tumor (5 d)	75 $\pm$ 14	87 $\pm$ 27	69 $\pm$ 14
Liver (7 d)	13 $\pm$ 4	19 $\pm$ 8	10 $\pm$ 5
Tumor (7 d)	77 $\pm$ 14	89 $\pm$ 31	65 $\pm$ 23

\*, the values are derived based on signal intensity, calibrated for iron concentration and iron/activity in the complex. SPECT, single photon emission computed tomography; MRI, magnetic resonance imaging.

Nuclear medicine systems do not provide the required resolution for dose estimation to metastatic small tumors accurately.

MRI is an anatomical imaging system with high-resolution and low-sensitivity images and the possibility to adjust the contrast to a desirable level (11,12,17). In this regard, MRI can be considered as complementary modality to scintigraphy because SPECT has high-sensitivity low-resolution images (10). Combination of these modalities can solve many problems related to RIT. One option available is making the hybrid systems to acquire co-registered and fused images. It was reported that using co-registration micro-positron emission tomography (microPET) with MRI images could confirm the position of  $^{86}\text{Y}$ -trastuzumab uptake relative to various organs. Their results demonstrated

the usefulness of combined microPET and MRI for the evaluation of novel therapeutics (11). In another study, microPET/CT and microMRI images were applied for *in vivo* evaluation of  $^{64}\text{Cu}$ -NO<sub>2</sub>A-8-Aoc-BBN(7-14)NH<sub>2</sub> in T-47D tumor-bearing mouse. The pharmacokinetic profile justifies investigation of this bioconjugate as a potentially useful diagnostic/therapeutic agent (23). Researchers applied the volume-rendered image, fused microSPECT/CT image from  $^{111}\text{Indium}$ -DOTA(GSGG)-G3-C12 for better detecting localization in the tumor and clearance from the renal/urinary pathway (24). In this study, we synthesized a dual radiopharmaceutical agent for therapy of breast cancer that could be followed by both SPECT and MRI systems. For better estimating the organs activity,  $^{177}\text{Lu}$ -trastuzumab was conjugated to iron oxide nanoparticles in order to be traced by MRI systems. Iron oxide nanoparticles are magnetic nanoparticles that produce a negative signal in their aggregation position. The main objective of this study was to determine the accumulated activity in organs in a new method by  $^{177}\text{Lu}$ -trastuzumab-iron oxide nanoparticles and MRI. The organ activity was determined with three different methods (MRI, SPECT imaging and tissue extraction) and compared with each other. The results showed very good correlation between the data derived MRI images and tissue extraction. So,  $^{177}\text{Lu}$ -trastuzumab-iron oxide nanoparticles with MRI had the ability to measure organ activity more accurately than with SPECT imaging and thus the dosimetry in this strategy could be performed more accurately than usual methods.

### Conclusions

$^{177}\text{Lu}$ -trastuzumab-iron oxide nanoparticles showed promising properties as a radioimmunoconjugate for better calculation of organs activity using MRI in mice bearing tumor. At this stage, we can conclude that the complex is potentially useful in providing high quality images for patient-specific dosimetry. However, further investigation is required to optimize the protocol of imaging and possibly better contrast agents should be used.

### Acknowledgements

*Disclosure:* The authors declare no conflict of interest.

### References

- Peña Y, Perera A, Batista JF. Immunoscintigraphy and



- radioimmunotherapy in cuba: experiences with labeled monoclonal antibodies for cancer diagnosis and treatment (1993-2013). *MEDICC Rev* 2014;16:55-60.
2. Yong KJ, Milenic DE, Baidoo KE, et al. 212Pb-radioimmunotherapy potentiates paclitaxel-induced cell killing efficacy by perturbing the mitotic spindle checkpoint. *Br J Cancer* 2013;108:2013-20.
  3. Maguire WF, McDevitt MR, Smith-Jones PM, et al. Efficient 1-step radiolabeling of monoclonal antibodies to high specific activity with 225Ac for  $\alpha$ -particle radioimmunotherapy of cancer. *J Nucl Med* 2014;55:1492-8.
  4. Kang GW, Kang HJ, Shin DY, et al. Radioimmunotherapy with (131I)-rituximab in a patient with diffuse large B-cell lymphoma relapsed after treatment with (90Y)-ibritumomab tiuxetan. *Nucl Med Mol Imaging* 2013;47:281-4.
  5. Seidl C. Radioimmunotherapy with  $\alpha$ -particle-emitting radionuclides. *Immunotherapy* 2014;6:431-58.
  6. Sendur MA, Aksoy S, Ozdemir NY, et al. The efficacy of adjuvant trastuzumab in HER-2 positive breast cancer with axillary lymph node metastases according to the treatment duration. *Curr Med Res Opin* 2014;30:2535-42.
  7. Siegel JA, Thomas SR, Stubbs JB, et al. MIRD pamphlet no. 16: Techniques for quantitative radiopharmaceutical biodistribution data acquisition and analysis for use in human radiation dose estimates. *J Nucl Med* 1999;40:37S-61S.
  8. Stabin MG, Sparks RB, Crowe E. OLINDA/EXM: the second-generation personal computer software for internal dose assessment in nuclear medicine. *J Nucl Med* 2005;46:1023-7.
  9. Dewaraja YK, Schipper MJ, Shen J, et al. Tumor-Absorbed Dose Predicts Progression-Free Survival Following 131I-Tositumomab Radioimmunotherapy. *J Nucl Med* 2014;55:1047-53.
  10. Giap HB, Macey DJ, Podoloff DA. Development of a SPECT-based three-dimensional treatment planning system for radioimmunotherapy. *J Nucl Med* 1995;36:1885-94.
  11. Palm S, Enmon RM Jr, Matei C, et al. Pharmacokinetics and Biodistribution of (86Y)-Trastuzumab for (90Y) dosimetry in an ovarian carcinoma model: correlative MicroPET and MRI. *J Nucl Med* 2003;44:1148-55.
  12. Woods RP, Mazziotta JC, Cherry SR. MRI-PET registration with automated algorithm. *J Comput Assist Tomogr* 1993;17:536-46.
  13. Yordanov AT, Hens M, Pegram C, et al. Antitnascin antibody 81C6 armed with 177Lu: in vivo comparison of macrocyclic and acyclic ligands. *Nucl Med Biol* 2007;34:173-83.
  14. Rasaneh S, Rajabi H, Babaei MH, et al. Radiolabeling of trastuzumab with 177Lu via DOTA, a new radiopharmaceutical for radioimmunotherapy of breast cancer. *Nucl Med Biol* 2009;36:363-9.
  15. Rasaneh S, Rajabi H, Hossein Babaei M, et al. Toxicity of trastuzumab labeled 177Lu on MCF7 and SKBr3 cell lines. *Appl Radiat Isot* 2010;68:1964-6.
  16. Rasaneh S, Rajabi H, Babaei MH, et al. MRI contrast agent for molecular imaging of the HER2/neu receptor using targeted magnetic nanoparticles. *J Nanopart Res* 2011;13:2285-93.
  17. Funovics MA, Kapeller B, Hoeller C, et al. MR imaging of the her2/neu and 9.2.27 tumor antigens using immunospecific contrast agents. *Magn Reson Imaging* 2004;22:843-50.
  18. Johnstone AP, Thorpe R. eds. *Immunochemistry in Practice*. Berlin: Wiley, 1996.
  19. Lindmo T, Boven E, Cuttitta F, et al. Determination of the immunoreactive fraction of radiolabeled monoclonal antibodies by linear extrapolation to binding at infinite antigen excess. *J Immunol Methods* 1984;72:77-89.
  20. Koyama Y, Barrett T, Hama Y, et al. In vivo molecular imaging to diagnose and subtype tumors through receptor-targeted optically labeled monoclonal antibodies. *Neoplasia* 2007;9:1021-9.
  21. van Reenen PC, Lötter MG, Heyns AD, et al. Quantification of the distribution of 111In-labelled platelets in organs. *Eur J Nucl Med* 1982;7:80-4.
  22. Gardin I, Bouchet LG, Assié K, et al. Voxeldoes: a computer program for 3-D dose calculation in therapeutic nuclear medicine. *Cancer Biother Radiopharm* 2003;18:109-15.
  23. Prasanphanich AF, Retzlaff L, Lane SR, et al. In vitro and in vivo analysis of [(64)Cu-NO2A-8-Aoc-BBN(7-14)NH(2)]: a site-directed radiopharmaceutical for positron-emission tomography imaging of T-47D human breast cancer tumors. *Nucl Med Biol* 2009;36:171-81.
  24. Schettino CJ, Kramer EL, Noz ME, et al. Impact of fusion of indium-111 capromab pendetide volume data sets with those from MRI or CT in patients with recurrent prostate cancer. *AJR Am J Roentgenol* 2004;183:519-24.

**Cite this article as:** Rasaneh S, Rajabi H, Johari Doha F. Activity estimation in radioimmunotherapy using magnetic nanoparticles. *Chin J Cancer Res* 2015;27(2):203-208. doi: 10.3978/j.issn.1000-9604.2015.03.06